

Validation of Dynamic 3-Dimensional Whole Heart Magnetic Resonance Myocardial Perfusion Imaging Against Fractional Flow Reserve for the Detection of Significant Coronary Artery Disease

Roy Jogiya, BSc, MBBS,* Sebastian Kozerke, PhD,*† Geraint Morton, MA, MBBS,* Kalpa De Silva, MBBS,‡ Simon Redwood, MD,‡ Divaka Perera, MD,‡ Eike Nagel, MD, PhD,* Sven Plein, MD, PhD*§
London, England; Zurich, Switzerland; and Leeds, United Kingdom

Objectives

The goal of this study was to determine the diagnostic accuracy of dynamic 3-dimensional (3D) whole heart myocardial perfusion cardiovascular magnetic resonance (CMR) against invasively determined fractional flow reserve (FFR) and to establish the correlation between myocardium at risk defined by using the invasive Duke Jeopardy Score (DJS) and noninvasive 3D whole heart myocardial perfusion CMR.

Background

3D whole heart myocardial perfusion CMR overcomes the limited spatial coverage of conventional two-dimensional perfusion CMR methods and allows estimation of the extent of ischemia. The method has shown good diagnostic accuracy for the detection of coronary artery disease (CAD) as defined by using quantitative coronary angiography. However, quantitative coronary angiography does not provide a functional assessment of CAD as available from pressure wire-derived FFR. In the catheter laboratory, the DJS can complement FFR to estimate the myocardium at risk.

Methods

Fifty-three patients referred for angiography underwent rest and adenosine stress 3D whole heart myocardial perfusion CMR at 3-T. Perfusion was scored visually on a patient and coronary territory basis, and ischemic burden was calculated by quantitative segmentation of the volume of hypoenhancement. FFR was measured in vessels with $\geq 50\%$ severity stenosis and an FFR < 0.75 considered as hemodynamically significant. The DJS was calculated from the coronary angiograms to quantify the myocardium at risk.

Results

FFR was measured in 64 of 159 coronary vessels, and 39 had an FFR < 0.75 . Sensitivity, specificity, and diagnostic accuracy of CMR for the detection of significant CAD were 91%, 90%, and 91%, on a patient basis and 79%, 92%, and 88%, respectively, by coronary territory. There was a strong correlation between the DJS and ischemic burden on CMR ($p < 0.0001$; Pearson's $r = 0.82$).

Conclusions

3D whole heart myocardial perfusion CMR accurately detects functionally significant CAD as defined by using FFR and provides an assessment of ischemic burden in agreement with the invasive DJS. The accurate detection of significant CAD combined with an estimation of ischemic burden by using 3D myocardial perfusion CMR holds promise for noninvasive guidance of therapy and risk stratification of patients with CAD. (J Am Coll Cardiol 2012;60:756–65) © 2012 by the American College of Cardiology Foundation

Cardiovascular magnetic resonance (CMR) is a rapidly evolving method for myocardial perfusion imaging (1,2). Compared with the more frequently used single-photon

emission computed tomography, CMR offers the advantages of higher in-plane spatial resolution and lack of ionizing radiation. In a recent, large, single-center study,

From the *King's College London BHF Centre of Excellence, NIHR Biomedical Research Centre and Wellcome Trust and EPSRC Medical Engineering Centre at Guy's and St. Thomas' NHS Foundation Trust, Division of Imaging Sciences, The Rayne Institute, London, United Kingdom; †Institute for Biomedical Engineering, University and ETH Zurich, Zurich, Switzerland; ‡King's College London BHF Centre of Excellence, NIHR Biomedical Research Centre at Guy's and St. Thomas' NHS Foundation Trust, Cardiovascular Division, The Rayne Institute, London, United Kingdom; and the §Multidisciplinary Cardiovascular Research Centre &

Leeds Institute of Genetics, Health and Therapeutics, University of Leeds, Leeds, United Kingdom. Dr. Plein is funded by British Heart Foundation fellowship FS/10/62/28409 and receives research grant support from Philips Healthcare. Dr. Kozerke receives funding from the Swiss National Science Foundation (grant number CR3213_132671/1) and research support from Bayer (Switzerland) AG. Dr. Nagel receives grant support from Bayer Healthcare and Philips Healthcare. All other authors have reported that they have no relationships relevant to the contents of this paper to disclose.

Manuscript received January 17, 2012; accepted February 23, 2012.

CMR had higher sensitivity and negative predictive value than single-photon emission computed tomography (3).

A limitation of myocardial perfusion CMR has been that the conventionally used two-dimensional (2D) acquisition methods cover the heart with a limited number (typically 3) of noncontiguous imaging slices.

See page 766

This selective coverage potentially limits diagnostic yield and impacts on the reliable quantitation of ischemic burden. More recently, three-dimensional (3D) myocardial perfusion CMR methods have been proposed to overcome the limitation of spatial coverage (4). 3D methods have shown good diagnostic accuracy for the detection of coronary artery disease (CAD) as determined by using quantitative coronary angiography (QCA) (5). Since the original reports on 3D myocardial perfusion CMR, technological advances have led to improved signal homogeneity, in particular at 3-T, and better reconstruction accuracy of temporally resolved signal intensity curves (6,7). These second-generation 3D methods have not been tested in a clinical setting. Furthermore, comparisons of myocardial perfusion imaging with QCA are inherently limited because of the variable relationship between the severity of coronary stenosis and its functional significance (8). A more appropriate validation of perfusion imaging can be made against invasive pressure wire-derived fractional flow reserve (FFR) measured during coronary angiography. FFR <0.75 correlates closely with objective evidence of reversible ischemia, and FFR-guided percutaneous coronary intervention confers a prognostic benefit (9).

Although one of the key advantages of FFR is that it is largely independent of vessel size and other confounders, this also implies that FFR provides no information on the extent of myocardium at risk, a separate marker of prognosis. For invasive estimation of ischemic burden, the Duke Jeopardy Score (DJS), which correlates the myocardium at risk with prognosis, has been described (10).

The objective of this study was to determine the diagnostic accuracy of a 3D whole heart myocardial perfusion CMR against FFR to detect flow-limiting coronary artery stenosis. A secondary aim was to establish the correlation between myocardium at risk defined by the DJS derived from angiographic data and ischemic burden as defined by the volume of hypoperfused myocardium on 3D whole heart myocardial perfusion CMR.

Methods

Patient population. The study was approved by the local research ethics committee, and all subjects gave written informed consent to participate. Fifty-five consecutive patients with known or suspected CAD were recruited before

clinically indicated invasive coronary angiography studies. Exclusion criteria were recent (<3 months) acute coronary syndromes, coronary artery bypass grafting, and contraindications to CMR imaging (including pacemakers and claustrophobia) or adenosine stress testing (poorly controlled obstructive airway disease and second- or third-degree atrioventricular block).

On the angiography procedure day, a full medical history was taken and a physical examination performed. Symptoms of chest pain were recorded in accordance with the Canadian Cardiovascular Society angina grading scale. A baseline electrocardiogram was performed and analyzed for the presence of Q waves or bundle branch block using defined Minnesota criteria (11).

CMR protocol. All subjects were scanned in the supine position on a 3-T magnetic resonance scanner (Achieva, Philips Healthcare, Best, the Netherlands) equipped with dual-source parallel RF transmission (MultiTransmit) technology (7) and a 6-channel cardiac phased-array receiver coil. Patients were monitored throughout the scan with a 4-lead vectorcardiogram, respiratory belt, and blood pressure monitoring. For perfusion imaging, a 3D spoiled turbo gradient-echo sequence was used (TR/TE/flip angle 1.8 ms/0.7 ms/15°; saturation prepulse delay 150 ms; acquisition timed to end-systole; partial Fourier acquisition; 10 fold *k-t* acquisition with 11 training profiles leading to a net acceleration of 7.0; *k-t* principal component analysis reconstruction [6]; reconstruction of 12 contiguous slices of 5-mm thickness; typical field of view 350 × 350 mm²; and acquired voxel size 2.3 × 2.3 × 5mm³).

Stress perfusion images were acquired during intravenous adenosine-induced hyperemia administered for 4 min at 140 μg/kg/min. An intravenous bolus of 0.075 mmol/kg of gadobutrol (Gadovist, Bayer Schering Pharma, Berlin, Germany) was administered at a rate of 4.0 ml/s followed by a 20-ml saline flush (Medrad Spectris Solaris power injector, Pittsburgh, Pennsylvania).

Stress perfusion CMR was followed by cine imaging covering the left ventricle in 10 to 12 short-axis sections and a rest perfusion scan performed 15 min later using the same concentration and volume of contrast agent (0.075 mmol/kg) as for stress perfusion. Late gadolinium enhancement (LGE) images (0.15 mmol/kg cumulative dose) were acquired in the same short-axis geometry after an additional 15 min using a conventional method (12).

Catheter laboratory protocol. FFR was calculated as: $(P_d - P_v)/(P_a - P_v)$, during hyperemia induced by infusion of intravenous adenosine at 140 μg/kg/min, where P_d ,

Abbreviations and Acronyms

- 2D** = two-dimensional
- 3D** = three-dimensional
- CAD** = coronary artery disease
- CI** = confidence interval
- CMR** = cardiovascular magnetic resonance
- DJS** = Duke Jeopardy Score
- FFR** = fractional flow reserve
- LGE** = late gadolinium enhancement
- QCA** = quantitative coronary angiography
- ROC** = receiver-operating characteristic

P_a , and P_v are mean distal coronary, aortic, and right atrial pressures, respectively (13). FFR was performed in all coronary arteries with luminal stenosis $\geq 50\%$ in 2 orthogonal views. FFR < 0.75 was considered to represent hemodynamically significant coronary stenosis. Vessels with chronic total occlusions were considered as significantly stenosed, and FFR measurements were not attempted. Angiographic images were analyzed quantitatively by using QCA (Medcon Ltd., Tel Aviv, Israel) by a blinded observer. Significant CAD was defined as $\geq 70\%$ diameter stenosis of the left anterior descending, circumflex, or right coronary arteries with ≥ 2 mm luminal diameter or $\geq 50\%$ diameter stenosis for the left main stem.

Duke Jeopardy Score. The DJS was calculated by using methods as originally described from myocardium at risk depending on the size and location (10). The coronary tree was divided into 6 segments of nearly equal myocardial perfusion (e.g., left anterior descending artery, major septal perforator, major diagonal branch, circumflex artery, major obtuse marginal branch artery, posterior descending artery). A score of 2 for each significant lesion was given; thus, a total maximal score of 12 could be derived. The cardiologists performing the coronary angiogram and all angiography-derived measurements were blinded to the CMR scan result.

CMR analysis. Two experienced observers, who were blinded to clinical details, visually analyzed the CMR images by using standard software (ViewForum, Philips Healthcare). Stress and rest perfusion scans and LGE images were viewed simultaneously. Image quality was graded on a scale from 1 to 4 (1 = uninterpretable, 2 = poor, 3 = good, and 4 = excellent). Image artifacts were recorded and categorized as breathing related, subendocardial rim artifacts, or related to the reconstruction of under-sampled data. A perfusion defect was considered present if reduced contrast uptake was seen at stress with $>25\%$ transmural in >1 contiguous slice persisting for >4 consecutive dynamic time points but not present at rest. Ischemia was only reported if the perfusion defect extended outside of any scar noted on matching LGE images. Perfusion defects were scored on a scale from 0 to 3 (0 = normal [all segments normal, no artifacts], 1 = probably normal [1 segment affected or suspected artifacts], 2 = probably abnormal [2 segments affected or artifacts], 3 = definitely abnormal [>2 segments affected and no artifacts]) for each perfusion territory to provide a summed stress score by each of the 2 observers. In case of disagreement, arbitration from a third observer was sought. For patient analysis, all normal and probably normal scores were classified as being normal and probably abnormal, and definitely abnormal scores were grouped as abnormal.

Perfusion defects were assigned to coronary territories by using the American Heart Association coronary arterial segment model (14). To simulate a comparison of 3D whole heart with 2D multislice myocardial perfusion CMR, only

slices 3, 7, and 11, representing apical, mid-myocardial, and basal sections, were reviewed in a separate analysis session, and reported a per-patient and per-vessel basis.

Ischemic volume calculation. The ischemic volume of myocardium was calculated by a separate blinded observer using GTVolume software (GyroTools Version 1.4, Zurich, Switzerland). A previously described method, which defines ischemic volume as tissue at an intensity threshold of <2 SDs below the signal of remote myocardium in the stress perfusion dynamic with the clearest delineation of a perfusion defect, was used (5). The total ischemic volume was calculated by summation of the hypoperfused areas in each slice. In patients with scar on LGE, scar volume was calculated in a similar fashion and peri-infarct ischemia was derived as the difference between the ischemia and scar volumes. The analysis was initially performed for all cases and then repeated for correctly identified cases only (i.e., excluding studies with false-positive and false-negative results).

To test reproducibility of detecting ischemic volumes, interobserver variability was assessed in a subset of 10 patients by a second reader fully blinded to clinical details and previous results. For intraobserver variability, the first reader repeated measurements of ischemic volumes 2 weeks later.

Statistical analysis. Data analysis was performed by using SPSS version 19.0 (SPSS Inc., Chicago, Illinois). Analysis was performed on both a patient and coronary territory basis to determine sensitivity, specificity, and negative and positive predictive values. These values were calculated for CMR to detect FFR < 0.75 . Receiver-operating characteristic (ROC) curve analysis was performed using the summed perfusion scores of the visual analysis. The interobserver variability of perfusion analysis was calculated using the kappa coefficient.

Interobserver and intraobserver variability of ischemic burden data, as determined with CMR, was calculated by using Bland-Altman analysis. Correlation between interobserver and intraobserver variability and the DJS and CMR ischemic burden was determined by using Pearson's test of correlation with a 2-tailed test of significance. For all analyses, $p < 0.05$ was considered significant.

Results

Patient population. Of the 55 patients recruited to the study, 1 study was incomplete because of claustrophobia and 1 was excluded because the CMR image quality was deemed uninterpretable. A total of 53 patients (41 men; mean age 63 years) thus formed the final population for analysis (Table 1).

Coronary angiography. Angiography was performed, on average, 2 days (range 0 to 14 days) after the CMR scan (Table 2). The overall disease prevalence in the study population was 64%. Of the 159 vessels analyzed, 72 (45%) vessels contained $\geq 50\%$ diameter stenosis on visual assess-

Table 1	Patient Demographic Characteristics (N = 53)
Male	41 (77.4)
Age (yrs)	63.5 ± 10.8
Range	43–83
BMI, kg/m ²	27.5 ± 4.1
Previous coronary intervention	14 (26.4)
Normal LV function	49 (92.5)
Canadian Cardiovascular Society Angina Grading Scale	
No pain or atypical symptoms	16 (30.2)
Class 1	24 (45.3)
Class 2	10 (18.9)
Class 3	3 (5.7)
Class 4	0 (0)
Baseline electrocardiogram	
Q-wave	4 (7.5)
Left bundle branch block	3 (5.7)
Right bundle branch block	1 (1.9)
Cardiovascular risk factors	
Diabetes	16 (30.2)
Dyslipidemia	44 (83.0)
Current smoker	9 (17.0)
Hypertension	35 (66.0)
Family history	20 (37.7)
Peripheral vascular disease	3 (5.7)
Medications	
Aspirin	51 (96.2)
Clopidogrel	19 (35.8)
Beta-blocker	35 (66.0)
Statin	50 (94.3)
Angiotensin-converting enzyme inhibitor or angiotensin receptor blocker	32 (60.4)
Nitrate	12 (22.6)

Values are n (%) or mean ± SD.
BMI = body mass index; LV = left ventricle.

ment. FFR was not performed in 2 of these vessels, which had heavily calcified long complex lesions, and in 6 vessels, which were either completely or subtotally occluded. These arteries were deemed significantly stenosed for the purpose of the analysis. FFR was performed in the remaining 64 arteries. Of these, 39 had an FFR <0.75 and 25 had an FFR ≥0.75. The total number of vessels with significant stenosis was thus 47. Twenty-four patients had single-vessel disease, 7 patients had 2-vessel disease, and 3 patients had 3-vessel disease as defined by a FFR <0.75.

QCA was retrospectively performed in all vessels and did not reveal any vessel with ≥50% stenosis that was not assessed by FFR. In the vessels with FFR ≥0.75, mean diameter stenosis was 48.7%; in vessels with FFR <0.75, diameter stenosis was 75.6%.

The mean FFR in vessels reported negative for ischemia by perfusion imaging was 0.82, (range 0.68 to 0.95; median 0.83) and the diameter stenosis in these vessels was 56.6%. The mean FFR in vessels reported as positive for ischemia by perfusion imaging was 0.61 (range 0.30 to 0.86; median 0.66) with a mean diameter stenosis of 71.7% (Fig. 1).

Table 2	X-ray Angiography Data
Time from CMR scan (days)	3.2 ± 3.3 (range 0–14; mode 0; median 2.0)
Resting systolic blood pressure (mm Hg)	128.7 ± 20.4
Resting diastolic blood pressure (mm Hg)	74.0 ± 12.9
Resting heart rate (beats/min)	66.5 ± 13.4
FFR systolic blood pressure (mm Hg)	121.3 ± 19.3
FFR diastolic blood pressure (mm Hg)	72.6 ± 11.4
FFR heart rate (beats/min)	81.0 ± 15.8
Vessels FFR measured (per patient)	1.2 ± 0.7
Vessels with FFR ≥0.75	25
Vessels with FFR <0.75	39
LAD	18
Cx	9
RCA	12
Patients with FFR positive*	
1-vessel disease	24 (45.3)
2-vessel disease	7 (13.2)
3-vessel disease	3 (5.7)
QCA in vessels with FFR ≥0.75 (% diameter stenosis)	48.7 ± 21.8
QCA in vessels with FFR <0.75 (% diameter stenosis)	75.6 ± 12.3

Values are mean ± SD, n, or n (%).
CMR = cardiovascular magnetic resonance; Cx = circumflex coronary artery; FFR = fractional flow reserve; LAD = left anterior descending coronary artery; RCA = right coronary artery; QCA = quantitative coronary angiography. *Includes 2 vessels with heavily calcified lesions and 6 vessels with chronic occlusion, in which FFR was not performed. These 8 vessels were deemed significantly stenosed.

Statistical significance was observed between the FFR of the 2 groups (p < 0.0001) and for QCA (p = 0.0013).

CMR imaging. Average examination time per patient was 51 ± 4 min. Typical symptoms were experienced in 46 of 53 patients during adenosine stress with mean blood pressure changing from 131/71 to 124/70 mm Hg (systolic p < 0.001; diastolic p = 0.16) and heart rates increasing from 68 to 81 beats/min (p < 0.01). Subendocardial LGE was found

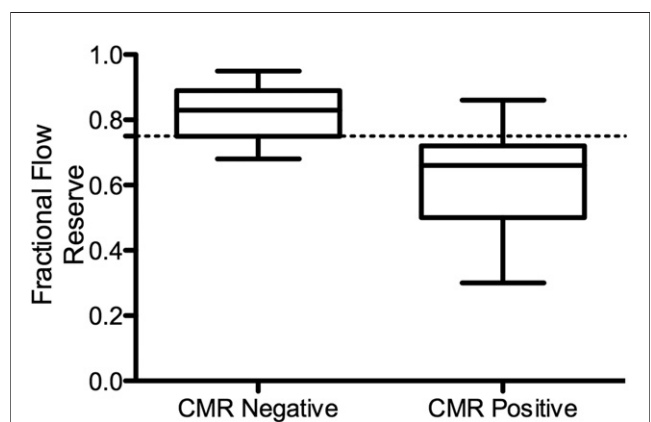


Figure 1 Box Plot Comparing FFR With 3D Whole Heart Myocardial Perfusion CMR

Relationship between three-dimensional (3D) whole heart myocardial perfusion cardiovascular magnetic resonance (CMR) versus fractional flow reserve (FFR) (64 coronary arteries). The mean FFR in the cohort is marked with a **dotted black line**: the mean FFR in coronary arteries with normal perfusion CMR was 0.82 versus a mean FFR of 0.61 in coronary arteries with abnormal perfusion CMR.

Table 3 CMR Data	
Scanning time (min)	50.8 ± 4.2 (range 42–66)
Resting systolic blood pressure (mm Hg)	131.1 ± 23.5
Resting diastolic blood pressure (mm Hg)	70.8 ± 12.7
Resting heart rate (beats/min)	67.9 ± 16.7
Stress systolic blood pressure (mm Hg)	124.5 ± 22.2
Stress diastolic blood pressure (mm Hg)	70.1 ± 11.4
Stress heart rate (beats/min)	81.1 ± 18.3
Image quality	3.1 ± 0.5
Artifact	
Breathing	8 (15.1)
Subendocardial rim	7 (13.2)
Adenosine symptoms	46 (86.8)
Adenosine complications	0
Late gadolinium enhancement	
Full-thickness	1 (1.9)
Partial-thickness	4 (7.5)

Values are mean ± SD or n (%).
 CMR = cardiac magnetic resonance.

in 4 patients, and a small area of transmural scar was seen in 1 patient. There was no significant difference in rest or stress hemodynamic data between 3D whole heart myocardial perfusion CMR and angiography (all p values >0.05) (Tables 2 and 3).

Image quality. The median image quality score was good (3.1 ± 0.5). The main artifacts seen were subendocardial dark rim–related artifacts in 7 patients (13%) and breathing artifact in 8 patients (15%), although the overall quality was deemed sufficient to make a diagnosis in all of these cases. Agreement between observers for the identification of abnormal perfusion per coronary territory showed a kappa of 0.94, indicating excellent agreement. In 4 patients (2.5% of coronary territories), a third reader was involved to arbitrate the remaining cases.

CMR analysis versus FFR. When analyzed per patient (Table 4), visual analysis of 3D whole heart myocardial perfusion CMR images yielded a sensitivity of 91.2% (95% confidence interval [CI]: 75.2 to 97.7), specificity of 89.5% (95% CI: 65.5 to 98.2), and diagnostic accuracy of 90.6% for

Table 4 Sensitivity and Specificity of 3D Whole Heart Myocardial Perfusion CMR Versus Coronary Angiography and FFR on Patient Basis			
CMR 3D Perfusion	Coronary Angiography/FFR		Total
	CAD Negative	CAD Positive	
Test positive	2	31	33
Test negative	17	3	20
Totals	19	34	53
95% Confidence Interval			
	Value	Lower Limit	Upper Limit
Prevalence	0.642	0.497	0.765
Sensitivity	0.912	0.752	0.977
Specificity	0.895	0.655	0.982

CAD = coronary artery disease; 3D = three-dimensional; other abbreviations as in Table 2.

the detection of significant coronary artery stenosis defined by a FFR <0.75. The positive predictive value was 93.9% (95% CI: 78.4 to 98.9) and the negative predictive value was 85.0% (95% CI: 61.1 to 96.0). ROC analysis showed an area under the curve of 0.89 (95% CI: 0.785 to 0.991; p < 0.0001). See Figure 2A for the ROC curve. Case examples are shown in Figures 3A and 3B.

When analyzed per vessel territory (Table 5), sensitivity was 78.7% (95% CI: 63.9 to 88.8), specificity was 92.0% (95% CI: 84.9 to 96.0), and diagnostic accuracy was 88.1%. The positive predictive value was 80.4% (95% CI: 65.6 to 90.1), and the negative predictive value was 91.2% (95% CI:

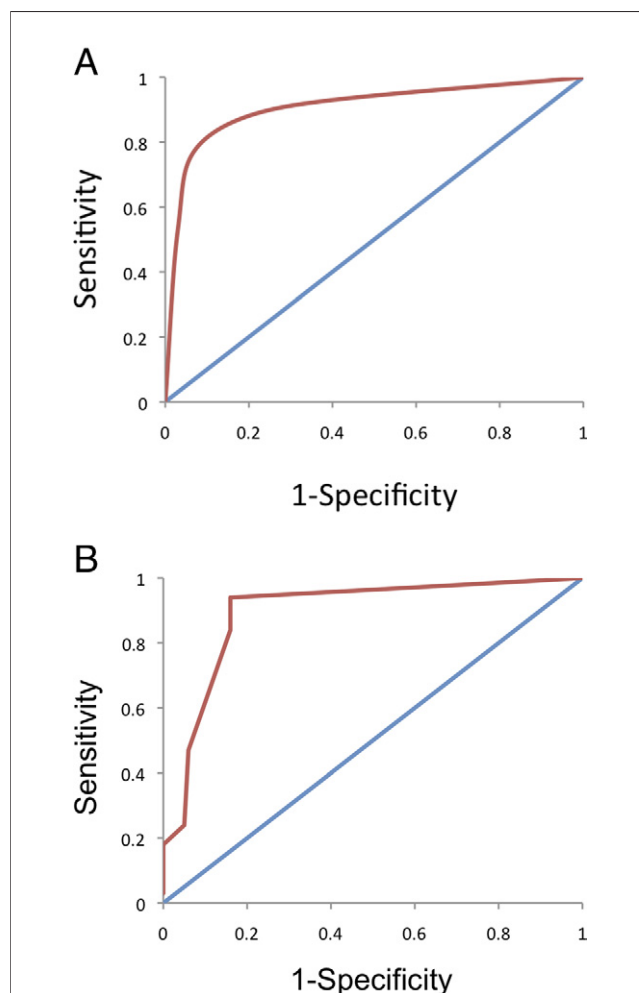


Figure 2 Receiver-Operating Characteristics Curves for 3D Whole Heart Myocardial Perfusion CMR Versus FFR for Patients and Coronary Territories

(A) Analysis per patient. Receiver-operating characteristic (ROC) curve showing sensitivity and specificity of the summed stress score of 3D whole heart myocardial perfusion CMR visual analysis to detect a hemodynamically significant coronary stenosis using a dichotomous value of 0.75 for FFR. The area under the curve was 0.89. (B) Analysis per coronary territory. ROC curve showing sensitivity and specificity of the summed stress score of 3D whole heart myocardial perfusion CMR visual to detect a hemodynamically significant coronary stenosis using a dichotomous value of 0.75 for FFR. The area under the curve was 0.88. Abbreviations as in Figure 1.

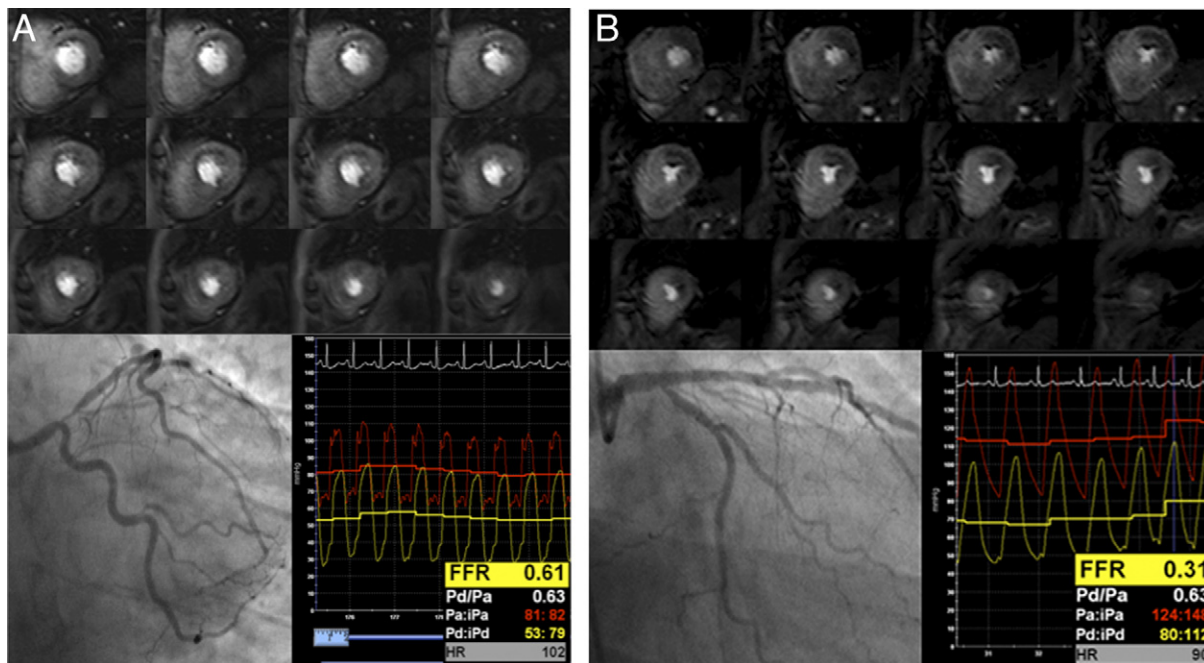


Figure 3 Case Examples: 3D Whole Heart Myocardial Perfusion CMR During Adenosine Stress Versus X-Ray Coronary Angiography and FFR

(A) A subendocardial defect is seen in the anterior and anteroseptal segments extending from the base to the apex. Invasive x-ray angiography demonstrated a proximal left anterior descending coronary lesion with an FFR of 0.61. (B) A transmural defect is seen from the lateral to inferolateral segments extending from the base toward the apex. Invasive x-ray angiography demonstrated an ostial circumflex coronary lesion with an FFR of 0.31. FFR = fractional flow reserve; HR = heart rate; Pa = aortic pressure; Pd = distal coronary pressure.

83.9 to 95.4). ROC analysis showed an area under the curve of 0.88 (95% CI: 0.801 to 0.994; $p < 0.0001$). Please see Figure 2B for the ROC curve.

When using only 3 slices of the whole heart perfusion datasets for analysis, the sensitivity, specificity, and diagnostic accuracy were 85.3% (95% CI: 68.2 to 94.4), 84.2% (95% CI: 59.5 to 95.8) and 84.9% on a patient basis. ROC analysis showed an area under the curve of 0.845. For the vessel analysis, sensitivity, specificity and diagnostic accuracy were 74.4% (95% CI: 59.4 to 85.6), 88.4% (95% CI: 80.6 to 93.4), and 84.3% with an area under the ROC curve of 0.81. None of these values were significantly different from the whole heart analysis.

CMR analysis versus QCA. Visual analysis of 3D whole heart myocardial perfusion CMR images, on a patient basis, yielded a sensitivity, specificity, and diagnostic accuracy of 87.9% (95% CI: 70.9 to 96.0), 80.0% (95% CI: 55.7 to 93.4), and 84.9%, respectively, for the detection of significant CAD defined by using QCA. These data are summarized in Table 6.

Ischemic burden versus DJS. The mean percentage ischemic volume (Table 7) on perfusion CMR was $9.9 \pm 10.9\%$. The mean DJS was 4.0 ± 3.9 . The mean percentage of ischemia volume for DJS of 0, 6, and 12 were 0%, 13.1%, and 36.7%, respectively. Figure 4 shows an example of the calculation of ischemia calculation.

Pearson's correlation coefficient showed a strong correlation ($r = 0.82$; 95% CI: 0.70 to 0.89) between the DJS and ischemic volume on CMR ($p < 0.0001$). If only patients correctly identified by using perfusion CMR (48 of 53) were included in the analysis, the correlation was stronger ($r = 0.87$; 95% CI: 0.78 to 0.93; $p < 0.0001$) (Fig. 5). Mean bias on Bland-Altman analysis was 0.1 ml (95% CI: -3.1 to 3.3) for intraobserver variability and 0.05 ml (95% CI: -1.8 to 1.9) for intraobserver variability. Pearson's correlation was very strong for both interobserver ($r = 0.96$) and intraobserver ($r = 0.98$) variability (Figs. 6A and 6B).

Discussion

This study found that 3D whole heart myocardial perfusion CMR accurately predicts the presence of hemodynamically significant coronary artery stenosis as measured by using FFR. In addition, it demonstrated close agreement between estimates of ischemic volume from 3D whole heart myocardial perfusion CMR and an invasive index of ischemic burden.

3D acquisition methods overcome some of the remaining limitations of myocardial perfusion CMR; specifically, the limited myocardial coverage offered by conventionally used 2D methods. Furthermore, 3D acquisition is more signal-to-noise efficient than 2D imaging; in addition, because all data are

Table 5	Sensitivity and Specificity of 3D Whole Heart Myocardial Perfusion CMR Versus Coronary Angiography and FFR on Coronary Territory Basis			
	CMR 3D Perfusion	Coronary Angiography/FFR		Totals
		Absent	Present	
Test positive	9	37	46	
Test negative	103	10	113	
Totals	112	47	159	
95% Confidence Interval				
	Value	Lower Limit	Upper Limit	
Prevalence	0.296	0.227	0.374	
Sensitivity	0.787	0.639	0.888	
Specificity	0.920	0.849	0.960	

Abbreviations as in Tables 2 and 4.

acquired in one shot, all images are acquired in the same cardiac phase. 3D myocardial perfusion CMR has become feasible as a result of recent advances in data acquisition speed, with several different methods proposed (4,15,16).

Following initial feasibility studies, a recent larger clinical study reported a sensitivity of 91.7% and a specificity of 74.3% of 3D myocardial perfusion CMR for the detection of coronary stenosis on QCA on a patient basis (5). However, QCA correlates poorly with the hemodynamic effect of a coronary stenosis because of effects of lesion proximity and length, calcification, collateral vessels, and dynamic changes in vasomotor tone (8). Pressure wire-derived FFR, which was the endpoint in the current study, is considered the reference standard for assessing the hemodynamic significance of atherosclerotic coronary lesions and is a more appropriate comparator for ischemia imaging than QCA.

Determining the functional significance of coronary stenosis is directly related to patient outcome, as shown for invasive assessment in the FAME and DEFER (9,17) cohorts and for noninvasive imaging in COURAGE and other studies (18–20). Furthermore, a substudy of FAME suggested visual and functional disparity, which highlights the need for functional assessment in patients with CAD (21). For these reasons, current guidelines recommend the use

Table 6	Sensitivity and Specificity of 3D Whole Heart Myocardial Perfusion CMR Versus Coronary Angiography and QCA on a Patient Basis			
	CMR 3D Perfusion	Coronary Angiography/QCA		Total
		CAD Negative	CAD Positive	
Test positive	4	29	33	
Test negative	16	4	20	
Totals	20	33	53	
95% Confidence Interval				
	Value	Lower Limit	Upper Limit	
Prevalence	0.642	0.497	0.765	
Sensitivity	0.879	0.709	0.960	
Specificity	0.800	0.557	0.934	

QCA = quantitative coronary angiography; other abbreviations as in Tables 2 and 4.

Table 7	Ischemia Volumes According to 3D Whole Heart Myocardial Perfusion CMR and Duke Jeopardy Scores (n = 53)				
	Score	LV Volume, ml	Ischemic Volume, ml	Myocardial Ischemia, %	DJS Score
Minimum	50.2	0.0	0.0	0.0	0
Median	68.0	8.1	11.5	11.5	4
Maximum	106.4	33.1	38.0	38.0	12
Mean	70.1	7.9	9.9	9.9	4.0
SD	12.3	8.0	10.9	10.9	3.9

DJS = Duke Jeopardy Score; LV = left ventricular.

of functional testing before elective revascularization (22). In clinical routine, however, fewer than one-half of patients are evaluated noninvasively before revascularization (23).

This study demonstrates excellent agreement between FFR and 3D whole heart myocardial perfusion CMR. Compared with the previous study, which compared 3D myocardial perfusion CMR with QCA, the specificity in the current analysis was higher (89.5% vs. 74.3%) whereas sensitivity was the same at 91% (5). The increased specificity of our analysis, reflecting a lower false-positive rate, is likely to relate to vessels that cause no functional flow limitation despite appearing significant on QCA. We observed a similar difference in specificity between the FFR and QCA analysis in the current study (89.5% vs. 80.0%).

In the current study, whole heart analysis did not statistically outperform the analysis of only 3 equally distributed slices of the 3D dataset, intended to simulate conventional 2D myocardial perfusion CMR methods. However, selecting 3 slices of a 3D dataset for analysis is not equivalent to the acquisition of a 3-slice 2D dataset. In a 3D dataset, all images are acquired in 1 optimized cardiac phase (systole in our study), which cannot be achieved in a multislice 2D acquisition. Conversely, 2D acquisition would yield a higher in-plane spatial resolution in a shorter acquisition time than 3D acquisition if a similar undersampling factor was applied. Further technical differences exist between 2D and 3D acquisitions that affect signal and contrast behavior of the acquired images. Our results can therefore only give an indication of the relative performance of 2D versus 3D myocardial perfusion CMR, and only an adequately powered head-to-head comparison of the 2 acquisition methods can provide conclusive evidence of their relative diagnostic performance. However, as demonstrated in this study, 3D acquisition has other advantages, in particular a more reliable estimation of ischemic volume.

We observed a strong correlation between ischemic burden on 3D whole heart myocardial perfusion CMR and the invasive DJS. Proximal lesions with a higher invasive score showed a higher volume of ischemia on CMR. Although not frequently used, invasive scores of ischemic burden have clinical legitimacy because the magnitude of myocardium at risk due to severe coronary stenosis is associated with an adverse prognosis (10,24,25), and isch-

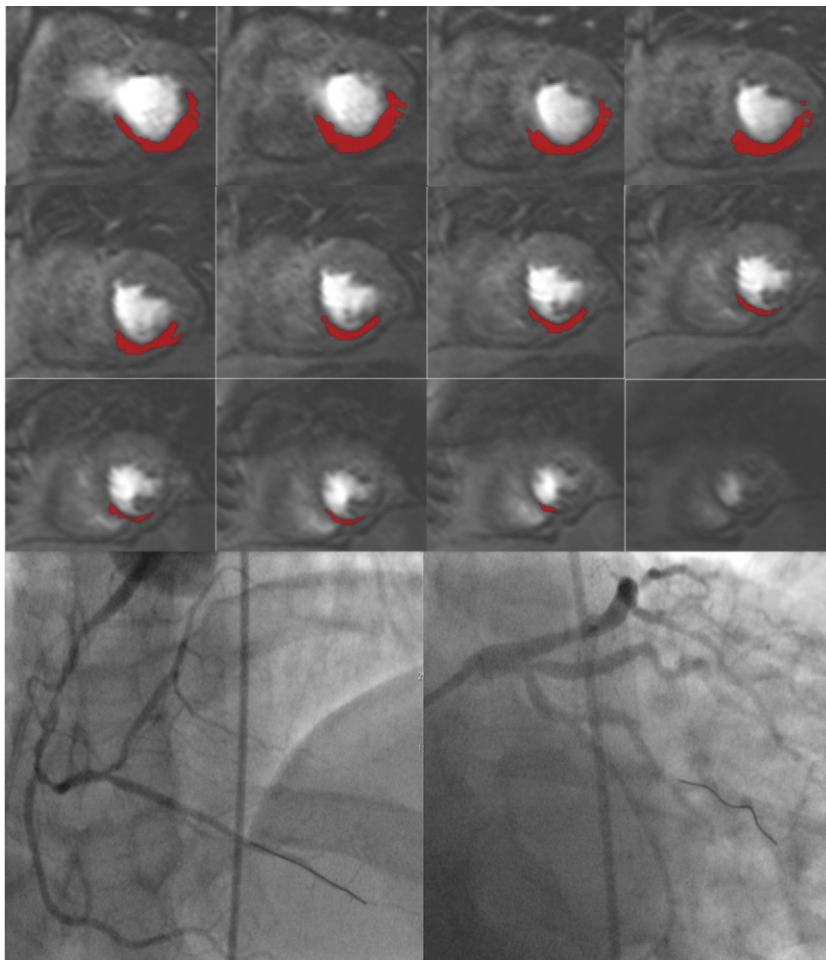


Figure 4 Case Example: 3D Whole Heart Myocardial Perfusion CMR During Adenosine Stress With Calculation of Ischemia Burden Versus Duke Jeopardy Score

A defect is seen in the inferior, inferoseptal, and inferolateral segments of >50% transmural extent from the base to apex. Invasive x-ray angiography demonstrating a proximal right coronary lesion with a fractional flow reserve of 0.67. The circumflex had a mid-course lesion with a negative FFR of 0.82. The ischemic volume was calculated as 12.3% of the myocardium (red). The area at risk calculated by using the Duke Jeopardy Score was 4. Abbreviations as in Figure 1.

emic burden is not reflected in the FFR. The DJS combines assessment of stenosis severity, location, and 5-year survival of patients with scores of <2, 6, and 12 of 97%, 85%, and 56%, respectively (10). Noninvasive assessment of myocardium at risk has similar prognostic relevance and an ischemic burden >10% to 12% may serve as a threshold at which revascularization conveys prognostic benefit over medical therapy alone (26).

Our study thus shows that 3D whole heart myocardial perfusion CMR allows both the detection of ischemia and provides an estimate of the extent of myocardium at risk. Such a noninvasive assessment may convey clinical advantages over invasive assessment. Compared with FFR-guided revascularization, noninvasive imaging is more suited for serial assessment and avoids potential iatrogenic complications, which could have economic implications, particularly in the multivessel setting (27). Although not formally assessed in the current study given the low prevalence of

prior myocardial infarction, the combination of 3D myocardial perfusion with LGE CMR will also permit a parallel assessment of ischemia and infarction in equivalent imaging planes, which is not possible with invasive assessment. A comprehensive assessment with 3D CMR methods thus holds promise as a noninvasive diagnostic and risk assessment tool for patients with known or suspected CAD.

Study limitations. This study investigated a population with a high disease prevalence. Future studies will be required to establish the diagnostic performance of 3D myocardial perfusion CMR in lower-risk patient groups. To minimize patient complications and to be consistent with clinical practice, FFR was only measured in vessels with $\geq 50\%$ coronary stenosis. It cannot be excluded that some lesions of <50% luminal stenosis may have had an abnormal FFR. We chose an FFR value of <0.75 as significant but recognize that the functional significance of “gray zone” FFR values (0.75 to 0.80) remains uncertain.

As in all studies comparing angiographic and imaging methods, we may not have correctly assigned all myocardial segments to the appropriate coronary artery. This limitation is likely to have accounted for some of the reduced sensitivity of per-vessel territory compared with per-patient analysis.

Both CMR and the DJS have limitations for the calculation of the ischemic burden. 3D whole heart myocardial perfusion CMR is a novel method, and no formal validation of estimates of ischemia volume with this method against a recognized reference test such as myocardial perfusion scintigraphy has been performed to date. The method of estimating ischemic volume from a single frame of the dynamic CMR data that was used in the current study and the previous report by Manka et al. (5) requires further validation. It should be noted that this method is not a substitute for quantitative estimation of myocardial blood flow, which has been used in other studies. Our analysis method provides a relatively fast but visual measurement of ischemic burden, whereas quantitative analysis methods of myocardial blood flow are more time-consuming but offer higher objectivity and the detection of balanced ischemia but have not yet been applied to 3D datasets.

The DJS has several limitations, including the difficulty of predicting the hemodynamic significance of coronary disease from angiography alone, particularly for intermediate lesions and the fact that it does not take into account myocardial viability. For this reason, we excluded any patients with a history of recent myocardial infarction (<3 months), but despite this 5 patients still had evidence of small infarcts on CMR. Furthermore, the DJS

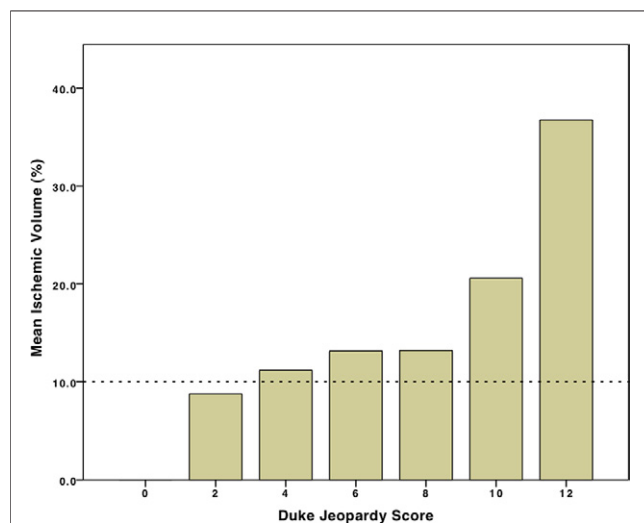


Figure 5 Correlation Between Ischemic Volume by 3D Whole Heart Myocardial Perfusion CMR Versus Duke Jeopardy Score (n = 48)

The dotted line indicates the 10% threshold cutoff previously quoted as being the point above which revascularization may confer prognostic benefit. For this graph only the 48 patients correctly identified by CMR were used.

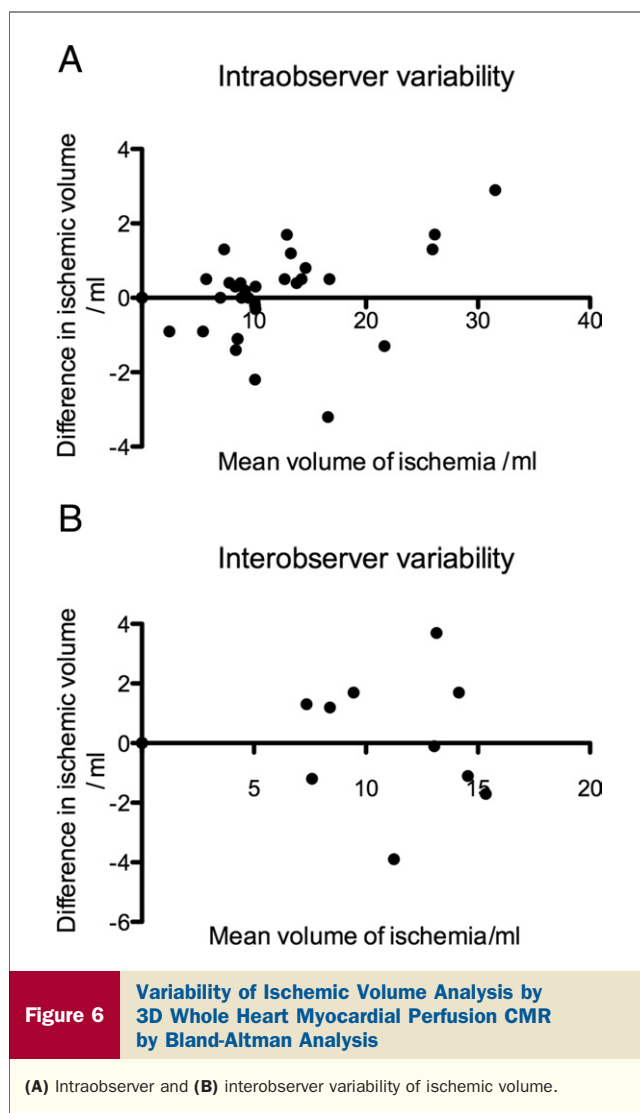


Figure 6 Variability of Ischemic Volume Analysis by 3D Whole Heart Myocardial Perfusion CMR by Bland-Altman Analysis

(A) Intraobserver and (B) interobserver variability of ischemic volume.

simply involves scoring the coronary tree segments and does not directly measure the size of the myocardial territory supplied by each vessel. This can cause problems with true left and right coronary artery co-dominance, unusual anatomic variations, and collaterization. However, although more precise scoring systems exist, they do not have the same attributes of simplicity and universal applicability.

Conclusions

3D whole heart myocardial perfusion CMR accurately detects functionally significant coronary artery disease with excellent sensitivity, specificity, and positive and negative predictive values when compared with FFR. CMR estimates of ischemic burden correlate closely with invasive DJS index. Multicenter studies to determine the use of 3D myocardial perfusion CMR as a noninvasive strategy for the diagnosis and risk stratification of patients with suspected CAD seem warranted.

Reprint requests and correspondence: Dr. Sven Plein, Multidisciplinary Cardiovascular Research Centre & Leeds Institute of Genetics, Health and Therapeutics, University of Leeds, G-floor, Jubilee Wing, Leeds General Infirmary, Leeds LS1 3EX, United Kingdom. E-mail: s.plein@leeds.ac.uk.

REFERENCES

1. Nandalur KR, Dwamena BA, Choudhri AF, Nandalur MR, Carlos RC. Diagnostic performance of stress cardiac magnetic resonance imaging in the detection of coronary artery disease: a meta-analysis. *J Am Coll Cardiol* 2007;50:1343–53.
2. Hamon M, Fau G, Née G, Ehtisham J, Morello R, Hamon M. Meta-analysis of the diagnostic performance of stress perfusion cardiovascular magnetic resonance for detection of coronary artery disease. *J Cardiovasc Magn Reson* 2010;12:29.
3. Greenwood JP, Maredia N, Plein S, et al. Cardiovascular magnetic resonance and single-photon emission computed tomography for diagnosis of coronary heart disease (CE-MARC): a prospective trial. *Lancet* 2012;379:453–60.
4. Shin T, Hu HH, Pohost GM, Nayak KS. Three dimensional first-pass myocardial perfusion imaging at 3T: feasibility study. *J Cardiovasc Magn Reson* 2008;10:57.
5. Manka R, Jahnke C, Paetsch I, et al. Dynamic 3-dimensional stress cardiac magnetic resonance perfusion imaging: detection of coronary artery disease and volumetry of myocardial hypoenhancement before and after coronary stenting. *J Am Coll Cardiol* 2011;57:437–44.
6. Pedersen H, Kozerke S, Ringgaard S, Nehrke K, Kim WY. k-t PCA: temporally constrained k-t BLAST reconstruction using principal component analysis. *Magn Reson Med* 2009;62:706–16.
7. Willinek WA, Gieseke J, Schild HH, et al. Dual-source parallel radiofrequency excitation body MR imaging compared with standard MR imaging at 3.0 T: initial clinical experience. *Radiology* 2010;256:966–75.
8. White CW, Wright CB, Marcus ML, et al. Does visual interpretation of the coronary arteriogram predict the physiologic importance of a coronary stenosis? *N Engl J Med* 1984;310:819–24.
9. Tonino PA, De Bruyne B, Fearon WF, et al., FAME Study Investigators. Fractional flow reserve versus angiography for guiding percutaneous coronary intervention. *N Engl J Med* 2009;360:213–24.
10. Califf RM, Phillips HR 3rd, Wagner GS, et al. Prognostic value of a coronary artery jeopardy score. *J Am Coll Cardiol* 1985;5:1055–63.
11. Rose GA, for the World Health Organization. *Cardiovascular Survey Methods*. 2nd edition. Geneva: World Health Organization, 1982.
12. Kim RJ, Wu E, Judd R, et al. The use of contrast-enhanced magnetic resonance imaging to identify reversible myocardial dysfunction. *N Engl J Med* 2000;343:1445–53.
13. Perera D, Biggart S, Redwood S, et al. Right atrial pressure: can it be ignored when calculating fractional flow reserve and collateral flow index? *J Am Coll Cardiol* 2004;44:2089–91.
14. Cerqueira MD, Weissman NJ, Dilsizian V, et al. Standardized myocardial segmentation and nomenclature for tomographic imaging of the heart: a statement for healthcare professionals from the Cardiac Imaging Committee of the Council on Clinical Cardiology of the American Heart Association. *Circulation* 2002;105:539–42.
15. Shin T, Pohost GM, Nayak KS. Systolic 3D first-pass myocardial perfusion MRI: Comparison with diastolic imaging in healthy subjects. *Magn Reson Med* 2010;63:858–64.
16. Vitanis V, Manka R, Kozerke S, et al. High resolution three-dimensional cardiac perfusion imaging using compartment-based k-t principal component analysis. *Magn Reson Med* 2011;65:575–87.
17. Pijls NH, van Schaardenburgh P, de Bruyne B, et al. Percutaneous coronary intervention of functionally nonsignificant stenosis: 5-year follow-up of the DEFER Study. *J Am Coll Cardiol* 2007;49:2105–11.
18. Jahnke C, Nagel E, Paetsch I, et al. Prognostic value of cardiac magnetic resonance stress tests: adenosine stress perfusion and dobutamine stress wall motion imaging. *Circulation* 2007;115:1769–76.
19. Shaw LJ, Berman DS, Boden WE, et al. Optimal medical therapy with or without percutaneous coronary intervention to reduce ischemic burden: results from the Clinical Outcomes Utilizing Revascularization and Aggressive Drug Evaluation (COURAGE) trial nuclear substudy. *Circulation* 2008;117:1283–9.
20. Sicari R, Pasanisi E, Venneri L, Landi P, Cortigiani L, Picano E; Group EPICES; Group EDICES. Stress echo results predict mortality: a large-scale multicenter prospective international study. *J Am Coll Cardiol* 2003;41:589–95.
21. Tonino PA, Fearon WF, Pijls NH et al. Angiographic versus functional severity of coronary artery stenoses in the FAME study fractional flow reserve versus angiography in multivessel evaluation. *J Am Coll Cardiol* 2010;55:2816–21.
22. Smith SC Jr, Feldman TE, Riegel B, et al. ACC/AHA/SCAI 2005 guideline update for percutaneous coronary intervention: summary article: a report of the American College of Cardiology/American Heart Association Task Force on Practice Guidelines (ACC/AHA/SCAI Writing Committee to Update the 2001 Guidelines for Percutaneous Coronary Intervention). *J Am Coll Cardiol* 2006;47:216–35.
23. Lin GA, Dudley RA, Redberg RF, et al. Frequency of stress testing to document ischemia prior to elective percutaneous coronary intervention. *JAMA* 2008;300:1765–73.
24. Graham MM, Faris PD, Knudtson ML, et al. Validation of three myocardial jeopardy scores in a population-based cardiac catheterization cohort. *Am Heart J* 2001;142:254–61.
25. Liao L, Lee KL, Mark DB, et al. A new anatomic score for prognosis after cardiac catheterization in patients with previous bypass surgery. *J Am Coll Cardiol* 2005;46:1684–92.
26. Hachamovitch R, Hayes SW, Friedman JD, Berman DS. Comparison of the short-term survival benefit associated with revascularization compared with medical therapy in patients with no prior coronary artery disease undergoing stress myocardial perfusion single photon emission computed tomography. *Circulation* 2003;107:2900–7.
27. Fearon WF, Bornschein B, Siebert U, et al. Economic evaluation of fractional flow reserve-guided percutaneous coronary intervention in patients with multivessel disease. *Circulation* 2010;122:2545–50.

Key Words: cardiovascular magnetic resonance imaging ■ fractional flow reserve ■ myocardial perfusion.